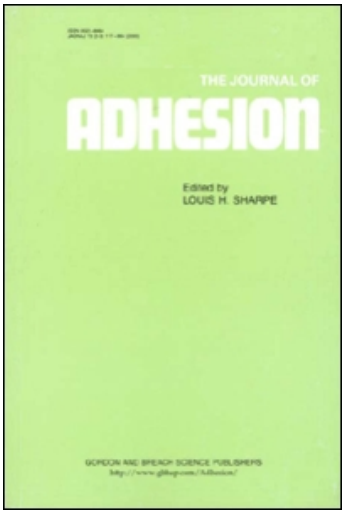

The Journal of Adhesion
Publication details, including instructions for authors and subscription information:
http://www.informaworld.com/smpp/title~content=t713453635

POLYELECTROLYTE MULTILAYERS AND THEIR INTERACTIONS

M. Müller[a]; J. Meier-Haack[a]; S. Schwarz[a]; H. M. Buchhammer[a]; K. -J. Eichhorn[a]; A. Janke[a]; B. Keßler[a]; J. Nagel[a]; M. Oelmann[a]; T. Reihs[a]; K. Lunkwitz[a]
[a] Institute of Polymer Research e.V., Dresden, Germany

Online publication date: 10 August 2010

To cite this Article Müller, M. , Meier-Haack, J. , Schwarz, S. , Buchhammer, H. M. , Eichhorn, K. -J. , Janke, A. , Keßler, B. , Nagel, J. , Oelmann, M. , Reihs, T. and Lunkwitz, K.(2004) 'POLYELECTROLYTE MULTILAYERS AND THEIR INTERACTIONS', The Journal of Adhesion, 80: 6, 521 — 547
To link to this Article: DOI: 10.1080/00218460490477189
URL: http://dx.doi.org/10.1080/00218460490477189

The Journal of Adhesion, 80: 521–547, 2004

ISSN: 0021-8464 print/1545-5823 online
DOI: 10.1080/00218460490477189

Taylor & Francis
Taylor & Francis Group

POLYELECTROLYTE MULTILAYERS AND THEIR INTERACTIONS

M. Müller
J. Meier-Haack
S. Schwarz
H. M. Buchhammer
K.-J. Eichhorn
A. Janke
B. Keßler
J. Nagel
M. Oelmann
T. Reihs
K. Lunkwitz
Institute of Polymer Research e.V., Dresden, Germany

An overview is given of our recent IR spectroscopic, optical, electrokinetic, and microscopic studies on polyelectrolyte multilayers (PEMs), built up using the consecutive layer-by-layer technique, their interactions, and application possibilities. The influence of pH on the deposition of PEMs consisting of commercial polyelectrolytes (PELs) like poly(ethyleneimine) and poly(acrylic acid) and the adopted surface morphology of isotropic PEMs consisting of flexible PELs are reported. PEMs of azo dye/PEL are included. Those are compared with anisotropic PEMs containing stiff PELs like charged α-helical polypeptides. Furhermore, examples concerning the swelling behavior of PEMs in the presence of solutions of different low molecular salt types and the hydration of dried PEMs by the relative humidity, respectively, are given. As potent application fields, their interaction with proteins regarding both prevention of bioadhesion and protein immobilization by electrostatic interaction forces are illustrated. Those studies led to

Received 27 November 2003; in final form 5 March 2004.

Financial support by the Deutsche Forschungsgemeinschaft (DFG: SFB 287, SPP 1009) is gratefully acknowledged.

One of a collection of papers honoring A. W. Neumann, the recipient in February 2004 of *The Adhesion Society Award for Excellence in Adhesion Science, Sponsored by 3M*.

Address correspondence to Martin Müller, Institute of Polymer Research (IPF), Department of Surface Modification, Hohe Str. 6, D-01069 Dresden, Germany. E-mail: mamuller@ipfdd.de

principles for membrane surface modification in order to prevent biofouling and optimize their flux and separation performance.

Keywords: Anisotropy; *In-situ* ATR-FTIR spectroscopy; Membranes; Protein adsorption; Polyelectrolyte multilayers; Surface modification; Swelling.

INTRODUCTION

Wet chemical surface modification by polyelectrolytes (PELs) is a classical processing step used in applications such as colloid stabilization and flocculation for water treatment and paper making [1, 2]. Currently, studies of PEL layers are underway to address novel application fields in nano- and bioscience, especially in sensor and biomaterial development. By applying thin to ultrathin layers, the already convenient performance of a material can be further improved. Besides chemical grafting [3, 4], PELs can be deposited from aqueous solutions on a variety of materials by simple adsorption techniques due to electrostatic interaction. For that, surface groups, which are already present or which can be introduced by several premodification techniques like plasma or chemical modification, can be used as anchors. Mainly three PEL-based modification concepts are applied by us, which are schemed in Figure. 1. Besides the single component adsorption (Figure 1a), *e.g.*, polycations at negatively charged surfaces, mixed systems of polycations (PCs) and polyanions (PAs) are progressively used in these applications (Figure 1b, and 1c). About ten years ago the concept of polyelectrolyte multilayers (PEMs; Figure 1b), making use of the consecutive adsorption of oppositely charged polyelectrolytes was introduced by Decher [5]. Using this concept of electrostatic self-assembly (ESA), coatings of defined and controlled thickness as well as morphological and chemical surface homogeneity can be generated on various kinds of surfaces, which

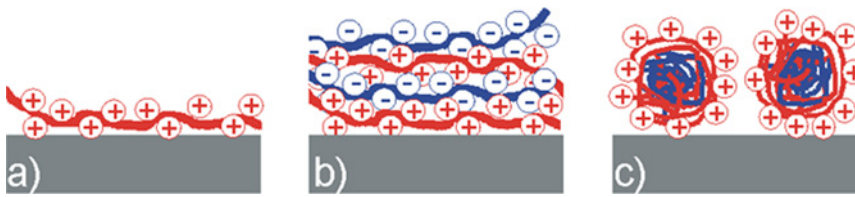

FIGURE 1 Concepts for the surface modification using polyelectrolytes (PELs): (a) single PEL component adsorption, (b) consecutive PEM adsorption, and (c) PEL complex (PEC) adsorption (See Color Plate I).

was comprehensively reviewed therein [6, 7]. Besides this concept, which shall be predominantly reported on here, the adsorption of preformed nonstoichometric nanoscopic PEL complexes (PECs; Figure 1c), prepared by mixing PC and PA in solution, can be applied [8–10]. This method is used to create defined nanoscopic surface structures like ordered arrangements of hemispheres, disks or wormlike particles [12]. Fundamental studies on PEL layer deposition at ideal and analytically well-accessible silicon surfaces are, on the one hand, used to relate the found phenomena to more applied yet complicated interfacial systems like dispersed particles, fibres, or membranes. On the other hand, since silicon is the substrate of choice in the semiconductor industry, PEL layers might become relevant for microelectronic chip processing. In particular, their capabilities for vertical and horizontal structuring, for binding (sensing, recognition), and for repelling (bio-inertness) are promising in that framework.

Here we report in an overview of our recent results on parameters and conditions for stable PEL layer systems and some results concerning their interaction with compounds of aqueous fluids close to application such as proteins. These studies serve the development of functional membranes [13, 14], carriers, sensors, and biomaterials [15–17].

EXPERIMENTAL

Polyelectrolytes

For the deposition of PEMs a limited number of PELs was used. As PCs branched, poly(ethyleneimine) (PEI; $M_w = 750.000\,g/mol$), poly (allylamine) (PAA; $M_w = 70.000\,g/mol$), poly(diallyldimethylammonium chloride) (PDADMAC; $M_w = 250.000\,g/mol$), and poly(L-lysine) (PLL; $M_w = 20.000$, 200.000, and $300.000\,g/mol$) were used (all from Sigma-Aldrich, Steinheim, Germany). They were combined with the PAs poly(acrylic acid) (PAC; $M_w = 90.000\,g/mol$, From Sigma Aldrich), poly(maleic acid-*co*-olefine-X) (PMA-X; X = P (propylene), MS (α-methylstyrene), $M_w = 23.000–50.000\,g/mol$, from Institute for Polymer Research Dresden, e.V., IPF, Dresden, Germany), poly(vinylsulfate) (PVS; $M_w = 160.000\,g/mol$, from Polyscience Washington, PA, USA), poly(styrene sulfonate) (PSS; $M_w = 70.000$ and $1.000.000\,g/mol$, Polyscience) and poly(L-glutamic acid) (PLG; $M_w = 70.000\,g/mol$, SigmaAldrich). Furthermore, anionic dyes like Direct Red 80 (DR 80) were combined with a weakly branched polycation containing 95% of N,N-dimethyl-2-hydroxypropyleneammonium

chloride units in the main chain ($M_w < 100.000$ g/mol, from S. Dragan, Institute of Macromolecular Chemistry, Iasi, Romania).

PEM Preparation

PEMs were prepared on different planar supports like silicon crystals, glass slides, or gold layers by consecutively injecting or cycling polycation and polyanion solutions in various *in situ* cells (1–5 ml) or by dipping, coating, and rinsing membrane materials. pH values of the PEL solutions were adjusted by carefully titrating with HCl or NaOH. The exposure time was between 10 and 20 min, followed by careful rinsing with water or salt solution used as the solvent for the previous adsorption step. Especially for the attenuated total reflection fourier transform infrared (ATR-FTIR) measurements, an automatic dosage system with valve control (IPF) was used for the deposition of PEMs in the *in situ* cell (IPF) at Si substrates. Occasionally, PEM films were dried below a gentle N_2 flow.

Methods

A broad spectrum of optical, spectroscopic, and microscopic surface analytical as well as wetting and electrokinetic methods can be applied to characterize PEMs. Especially, atomic force microscopy (AFM), ellipsometry, surface plasmon resonance (SPR), and *in situ* ATR-FTIR spectroscopy deliver information concerning surface morphology, film thickness, molecular composition, conformation, and orientation of layer compounds.

Ellipsometric measurements were performed by *in situ* spectroscopic ellipsometry in a spectral range from 428–763 nm using a variable angle multiwavelength ellipsometer M-44 (J. A. Woollam Co., Lincolna, NE, USA).

SPR data were recorded by a homebuilt apparatus (J. Nagel, IPF Dresden) consisting of a He-Ne laser (632.8 nm, Uniphase, IDS Uniphase, San Jose, CA, USA), a semicylinder made of SF10 glass (coupled to SF10 gold coated glass slide), a liquid flow cell with the volume of 2.5 ml, and a photodiode detector with an integral preamplifier (Linos GmbH, Göttingen, Germany). The data were fitted according to Fresnel's equations for a four-layer model (glass/metal/dielectric/surrounding medium)[18].

The AFM experiments were carried out with a Dimension TM 3100 system (Digital Instruments, Woodbury, NY, USA) in the noncontact mode. The tip used for the experiments was a silicon probe from Nanosensors (Darmstadt, Germany).

For the ATR-FTIR measurements a special mirror setup operated by the single beam sample reference (SBSR) regime (OPTISPEC, Prof. U.P. Fringeli, Zürich, Switzerland) [19] and an *in situ* ATR-FTIR double channel flow cell (M. M., IPF Dresden) was used within a commercial FTIR spectrometer (IFS 55 Equinox, BRUKER-Saxonia, Leipzig). This allowed for flat baseline and proper compensation of background signals (absorptions from water vapor, bulk water, and crystal material) in the recorded ATR-FTIR spectra.

RESULTS AND DISCUSSION

The internal structure of PEMs is actually under intense discussion. It is commonly accepted that PEMs exhibit a defined excess surface charge depending on the last adsorbed layer and that PEMs do not show stratified layer structures as was scoped in an early phase of the PEM concept [5]. Moreover, the internal structure of ordinary PEMs like those of the flexible PELs poly(allylamine) and poly(styrene sulfonate) or poly(acrylic acid) are claimed to be in a fuzzy disordered state [20–22], so that high overlapping of the individual layers and high entanglement prevails. Nevertheless, the stratification of the individual layers is an interesting task and can be achieved by several approaches. The PEMs studied within that review may be classified in the following way: PEMs consisting of the flexible PELs PEI, PAC, PVS, PMA-X, dyes, and also proteins are denoted as isotropic PEMs. PEMs of stiff PELs, such as charged α-helical polypeptides [23], but also layered silicates [24] or ionenes [25], do form anisotropic PEMs.

Isotropic PEMs

pH Dependence

PEMs consisting of the two pH-dependent—*i.e.*, weak—PELs, PEI and PAC, have become a standard system in our research. In Figure 2a typical *in situ* ATR-FTIR spectra monitoring consecutive PEI/PAC deposition are shown [26]. With increasing number of adsorption steps x (PEM-x) the intensity of the ATR-FTIR spectra grows. Up to thicknesses, d, of about 300 nm the ATR measured absorbance of PEL marker bands, proportional to the adsorbed amount, is approximately linear with the adsorption step, x. For higher d values the signal increase takes an asymptotic course due to an exponentially damped function of A *versus* x [26].

In Figure 2b the course of the integrated absorbance of the ν(OH) band ($A_{\nu(OH)}$) is shown for various pH combinations (pH = 9/4, 4/4, and 9/9 for PEI/PAC) of the PEI and PAC solution. The decrease of

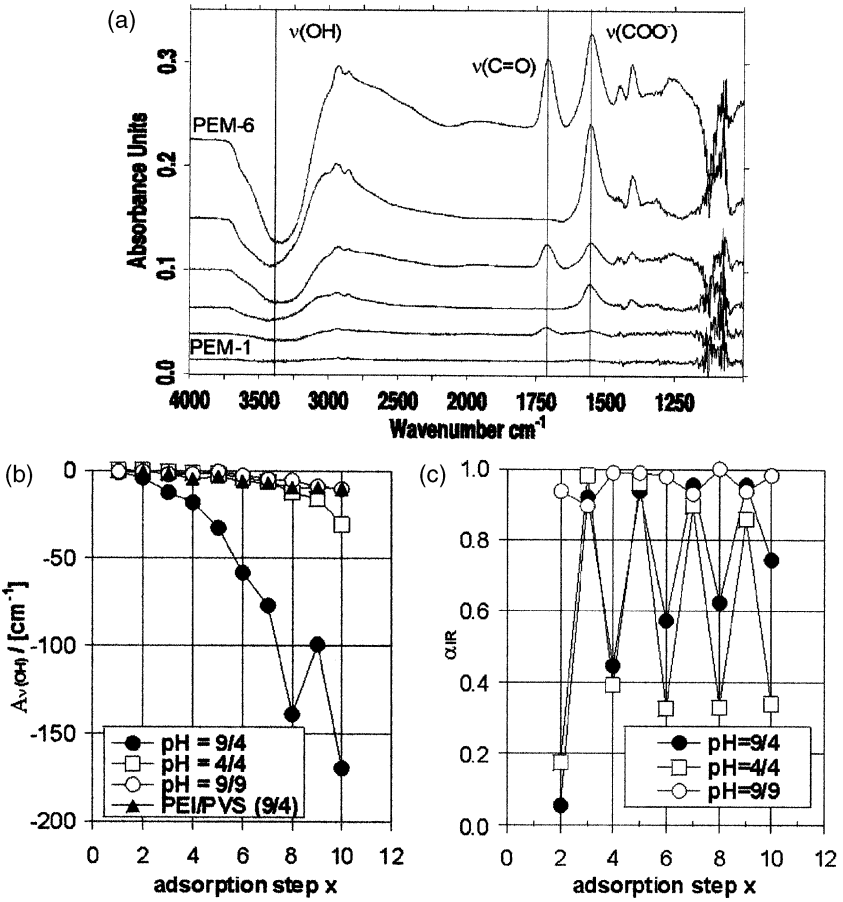

FIGURE 2 (a) In situ ATR-FTIR spectra on the consecutive PEI/PAC deposition (c = 0.01 M, pH = 9 (PEI) 4 (PAC)) from solution onto Si-ATR crystals (from Müller [26], with kind permission of Wiley-VCH). (b) Adsorbed amounts of the PEM-PEI/PAC at Si-supports as a function of the adsorption step x for the pH combinations 9/4 (●), 4/4 (□), and 9/9 (○), and of the PEM of PEI/PVS at pH = 9/4 (▲). (c) Dissociation degree α_{IR} of PEM-PEI/PAC at Si-supports as a function of x for the pH combinations 9/4 (●), 4/4 (□), and 9/9 (○).

the $A_{\nu(OH)}$ reflects the replacement of water at the support surface with the deposited PEM and is a measure of the adsorbed PEM amount. Significantly, the combination of pH = 9/4 revealed the highest adsorbed amount, since both PEI and PAC possess only a few charged groups due to deprotonation. This causes the PEL to adopt a coiled conformation, leading to thick films of loopy internal

structure. For the combination pH = 4/4 a smaller, and for pH = 9/9 the smallest, adsorbed amount was found, since in those cases at least one PEL component is fully charged and should form an extended structure of the PEL chain due to electrostatic repulsion of the charged monomer segments.

For further studies on the deposition mechanism of PEMs the dissociation degree, α_{IR}, of the weak polyacid PAC is useful [26, 27]. Access to α_{IR} of PAC can be obtained by the absorbance of the ν(C=O) and the $\nu(COO^-)$ band due to carboxyl and carboxylate groups, respectively, *via* Equation (1) [26]:

$$\alpha_{IR} = \frac{A_{\nu(COO^-)}}{A_{\nu(COO^-)} + 1.74 \cdot A_{\nu(C=O)}}. \quad (1)$$

A modulated course between $\alpha_{IR} = 1$ for the PEI steps and a lower value of the following PAC steps, which are subsequently increasing, is obtained for the setting pH = 9/4 by plotting α_{IR} *versus* the adsorption step, x, in Figure 2c. This reflects the layer-by-layer overcharging of the PEM in every step, where in all PEI steps all underlying COOH groups are deprotonated, and in all PAC steps new COOH groups for the next PEI binding are exposed. The α_{IR} of PAC approaches 1, since with increasing step numbers the last layer contributes subsequently to a minor extent to the α_{IR} of the total PEM. From that a 1:1 charge compensation between PC and PA as well as the absence of counterions in the PEM interior can be concluded. For pH = 4/4 in the PEI steps all COOH groups are reacted ($\alpha_{IR} = 1$) in spite of the acid pH, and in the PAC steps slightly more unreacted COOH groups remained in comparison with 9/4. For pH = 9/9 in both PEI and PAC steps $\alpha_{IR} = 1$ means that PAC was fully dissociated, which caused the thinner layers.

Influence of the Polyanion

In comparison with the PEM of PEI/PAC, those of PEI/PVS led to smaller adsorbed amounts for the pH combination 9/4 (Figure 2b). This was caused by the higher charge density of the PVS compared with PAC, leading to a more extended conformation of PVS and, therefore, to thinner adsorbed layers.

Influence of the Molecular Weight

Another important parameter influencing PEM deposition is the molecular weight (M_w) of one or both PEL components. Solutions of two poly(styrene sulfonate) (PSS) samples with high (PSS(h), 1,000,000 g/mol) and low (PSS(l), 70,000 g/mol) molecular weight

were consecutively adsorbed with PEI. SPR, which is based on the change of the resonance angle as a function of the thickness and the refractive index of the sample layer deposited onto gold-covered glass supports, was used. This is principally shown for PEM of PEI/PSS(l) in Figure 3a, where a diagnostic shift of the resonance angle from $57^\circ - 75^\circ$ can be observed as a function of the number of double layers (n(dl) = 2x). In Figure 3b the fitted thicknesses of the series PEI/PSS(l) and PEI/PSS(h) are presented as a function of the number of double layers. The thickness was obtained from the best fit of a four-layer model to the data using a refractive index of n = 1.5 [18], which is approximately supported by scanning angle reflectometry (SAR) measurements resulting in n = 1.48–1.49 [21, 28].

The thickness of the PEM-10 was approximately 150 nm for PEI/PSS(h) and 25 nm for PEI/PSS(l). This can be explained by the larger coil radius of PSS(h) compared with PSS(l) in solution, resulting in higher adsorbed amounts and thickness when consecutively adsorbed at the surface.

Isotropic PEM Surface Morphology

Up to now information from the literature on lateral structures of isotropic PEMs does not form a clear picture. According to Schlenoff, planar PEMs of PDADMAC/PSS exhibit unexpectedly rough and inhomogeneous surfaces but can be smoothed by the addition of salt [29]. Taking reference on that finding PEMs consisting of poly (allylamine) (PAA)/poly(4-styrenesulfonate) (PSS) were deposited on Si wafers and were studied by ellipsometry and scanning force microscopy (SFM). Figure 4a shows the SFM micrograph of the PEM PAA/PSS-11, and Figure 4b shows the absolute thickness and roughness (RMS) values as a function of the adsorption step x (x = 7, 9, 11, 15).

Significantly, the PEM-11 shows granular structures on the surface, the morphology, of which is quite similar to that of adsorbed preformed polyelectrolyte complexes [11]. Presumably, they can form in the following manner: onto isolated and inhomogeneously adsorbed polycations of the first step, both laterally and vertically polyanions and oppositely charged PEL are adsorbed consecutively. Thereby individual piles are formed on the surface, which are laterally fusing with increasing adsorption steps (growing into one another). Presumably, from PEM-9 forward, complete layers are formed, which can be shown by the decrease of the RMS roughness from PEM-7 (6.4 nm) to PEM-9 (4.1 nm) and a similar value at PEM 11 (4.2 nm) shown in Figure 4b. Further consecutive layer deposition from PEM-11 to PEM-15 (7.3 nm) results in a roughness increase, presumably caused by the

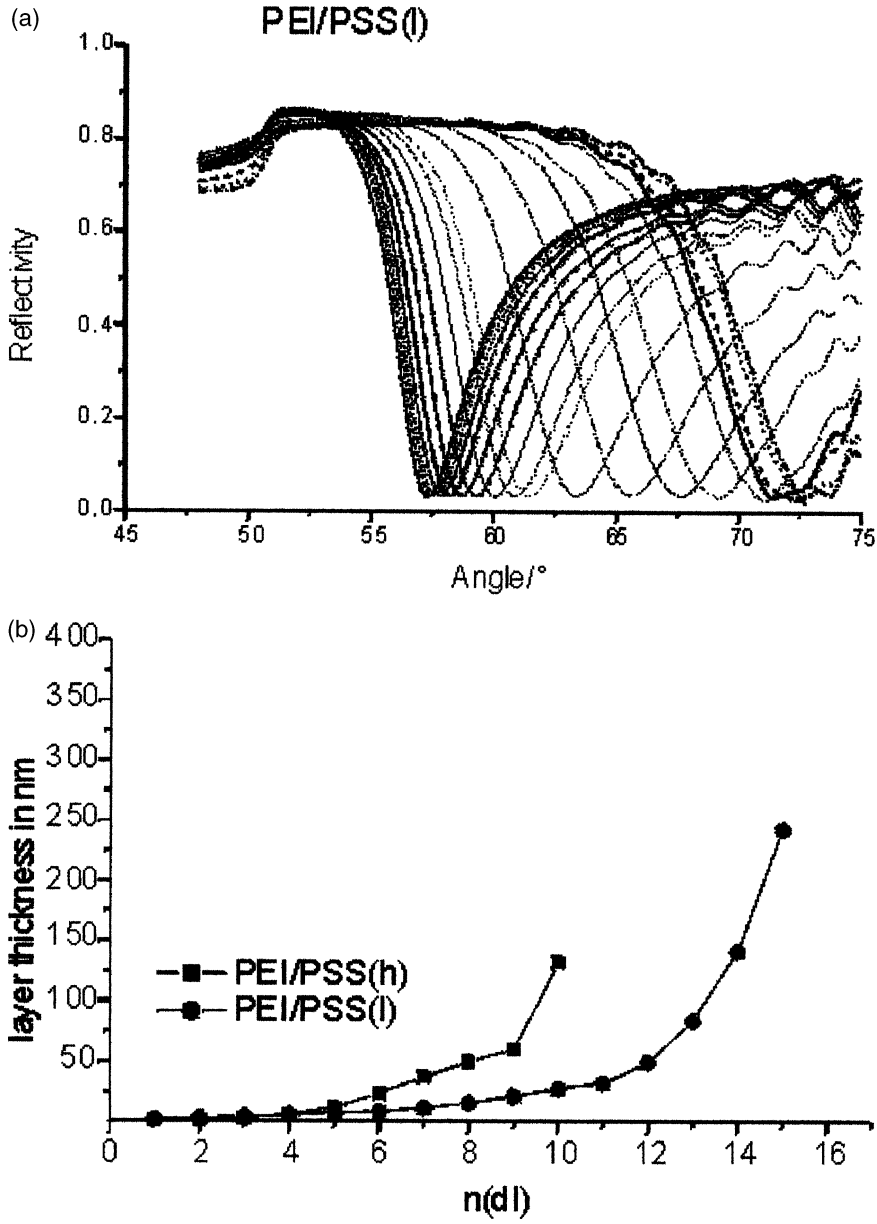

FIGURE 3 (a) SPR curves measured after the adsorption of PEI/PSS(l) double layers in water. Shift of the SPR minimum to higher angles from 0 to 20 double layers in water (from Schwarz *et al.* [18] with kind permission of Wiley-VCH). (b) Courses of the layer thickness as a function of the number of double layers (n(dl)) for PEI/PSS(l) and PEI/PSS(h). The thickness was based on a four-layer fit (from Schwarz *et al.* [18], with kind permission of Wiley-VCH).

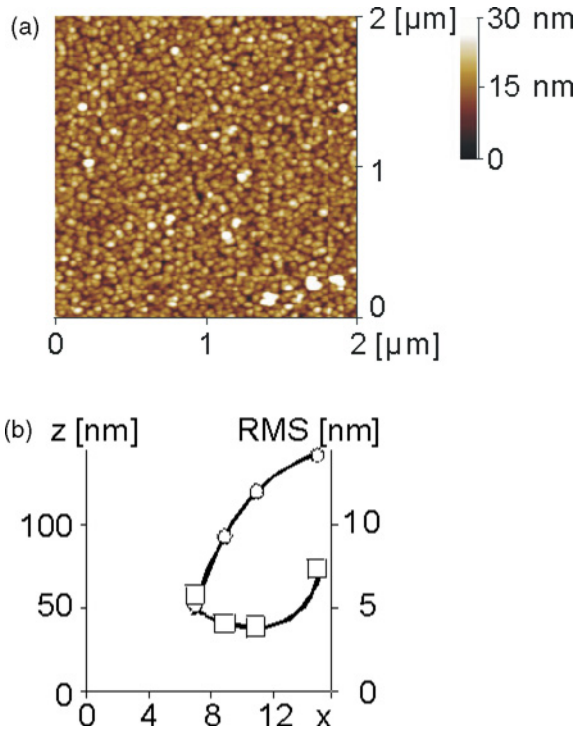

FIGURE 4 (a) SFM micrograph of PEM-11 consisting of PAA/PSS on the Si wafer (See Color Plate II). (b) Dependence of the ellipsometric layer thickness,

formation of new piles. Also, in the increment between PEM-11 (121 nm) and PEM-15 (143 nm) the approximate linear increase of the ellipsometric thicknesses, d, from PEM-7 (52 nm), and PEM-9 (94 nm) to PEM-11, seems to stop, which might be also a hint for an inhomogeneous film growth now more in the vertical than in the horizontal direction. This is under further investigation.

Polyelectrolyte/azo Dye Multilayers

Using the layer-by-layer approach charged dyes could also be incorporated in self-assembled nanoarchitectures, as was already shown in [30–32]. Although the building up of the polyelectrolyte-dye multilayers seems very simple to achieve, the influence of the polyion and of the dye structure on the molecular and supramolecular organization is still not understood. Recently, PEMs consisting of a polycation

containing 95% N,N-dimethyl-2-hydroxy-propyleneammonium chloride repeat units (PCA_5) and various multicharged azo dyes were reported [33, 34]. Among them Direct Red 80 (DR 80), which carries six sulfonate groups ($pK < 1$), was consecutively deposited with PCA_5 from saltless aqueous solutions on glass substrates. This was followed by UV absorbance as a function of the double layer number, n(dl), and by ζ-potential measurements introduced for PEMs on planar substrates in [35].

Figure 5a shows the increase of the absorbance at 558 nm as a function of n(dl), where the position of the maximum remained the same irrespective of n(dl) suggesting a regular uptake of the dye into the PEM. Additionally, ζ-potential measurements were performed in order to probe the surface charge properties of those PEMs. In the Figure 5b the ζ-potential is plotted against pH for PEMs of PCA_5/DR80 with different layer numbers (PEM-4, PEM-5, PEM-10, and PEM-11) adsorbed in the presence of 1 M NaCl on glass slides. Generally, the pH value at which the ζ-potential is zero gives the isoelectric point (IEP) of the surface, and the ζ-potential value is a measure of the surface charge. Firstly, PEM-4 and PEM-10 resulted in IEP = 4.3, whereas PEM-5 and PEM-11 resulted in a shift to IEP = 5.5. This qualitatively reflects the anionic surface charge for the DR80-terminated PEMs and the significant shift to less anionic surface charge for the PCA_5-terminated PEM, which is caused by ion pairing between the sulfonate and ammonium groups of DR80 and PCA_5, respectively. The fact that the IEP of the DR80-terminated PEMs are higher and of the PCA_5-terminated PEMs are lower compared with the IEP of those components in solution is caused by segments of the respective underlying component penetrating into the outermost one.

Secondly, both the IEP and the ζ-potential amplitudes were about independent on the layer number. First, this reflects the stability of the PEM under the streaming potential measurement conditions. Second, it shows that the outermost layer exclusively determines the sign and the amplitude of the surface charge and thus the ability to bind a new polycation or dye layer in a reproducible manner independently of the absolute layer number.

Anisotropic PEMs

In the previous section, PEMs were introduced showing more or less isotropic internal structure, which is, in our opinion, the rule using flexible polycations and polyanions. Recently, in contrast to that, it could be shown that PEMs consisting of stiff PELs such as charged

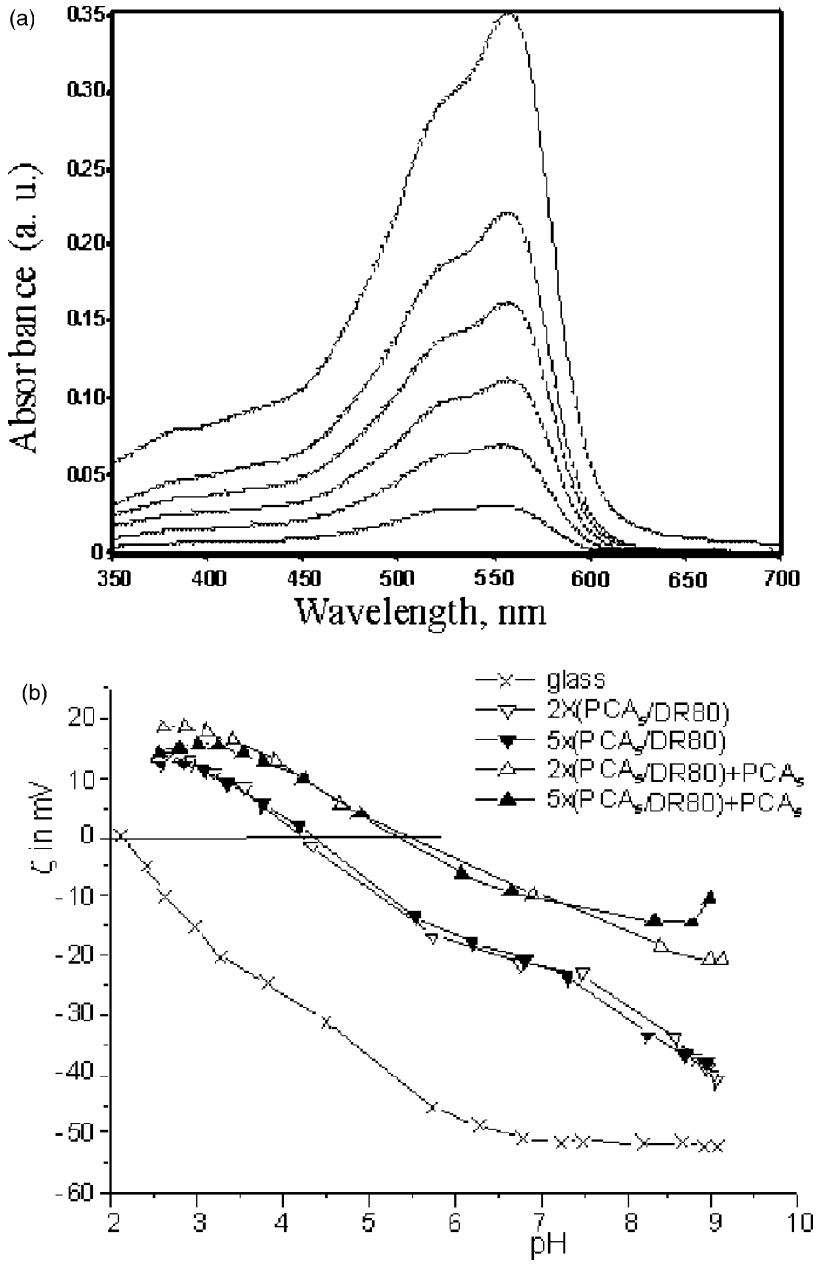

FIGURE 5 (a) UV/VIS spectra on the consecutive deposition of PCA_5 and DR 80 as a function of n(dl). Spectra recorded for n(dl) = 1–6 from bottom to top are shown (from Dragan *et al.* [33], with kind permission of Elsevier). (b) ζ-potential/pH profiles for the glass support, PEM-4/5 and PEM-10/11 of PCA_5 and DR 80 (from Dragan *et al.* [33], with kind permission of Elsevier).

α-helical polypeptides showed anisotropic properties [23, 36]. This could be proven by dichroic ATR-FTIR spectroscopy on PEMs containing PLL or PLG in their α-helical state, respectively.

PEMs consisting of charged homopolypeptides are currently finding high interest since distinct stable internal secondary structures can be generated as was shown by the Strassbourg PEM group [37–39]. Our approach has been to bring the cationic polypeptide PLL as well as the anionic PLG in to the α-helical conformation by certain salt and pH settings and to deposit them consecutively with strong oppositely charged polyelectrolytes. To orient those PEMs texturized substrates exhibiting parallel grooves of 50–70 nm width and 5–8 nm depth were used [23, 36]. In the Figure 6a p- and s-polarisation ATR-FTIR spectra of the PEM of α-PLL/PVS and in Figure 6b of α-PLG/PDADMAC are shown. The principle of dichroic ATR-FTIR spectroscopy and the application on oriented multilayers is given in Müller *et al.* [36]. IR dichroism is based on the different absorption of linearly polarized light by oriented chromophors. Principally, parallel (p) and vertical (s) polarized IR light cause different absorbances, A_p and A_s, of characteristic IR bands, where the dichroic ratio $R = A_p/A_s$ is a direct measure of the orientation state of the given band. Knowing the position (angle Θ) of this band relative to a molecular axis, it is possible to determine the molecular orientation.

In both cases (Figure 6a and 6b) dichroic ratios of $R^{ATR} < 1$ for the amide I and $R^{ATR} >> 1$ for the amide II band, which is diagnostic for in-plane unidirectional alignment, were obtained (R^{ATR} values obtained by ATR mode were transformed into R values accessible by transmission mode as described in Müller [23]). Knowing the angle θ between the transition dipole moment of the amide vibrations (Amide I: 38°, Amide II: 73° [40]) and the molecular axis, an order parameter, S, in the sense of unidirectional alignment, could be quantitatively determined using Equation (2) [36]. Thereby, $S = 0$ means no, $S = 1$ means high parallel, and $S = -1/2$ means high vertical uniaxial orientation with respect to the groove (orientation) direction. This orientation analysis is based on the model of a cone, which is formed by the molecular axes of oriented molecules [41], in our case the α-helical polypeptides. The cone opening angle, γ_0, is directly related to S by Equation (3), where $\gamma_0 = 0$ ($S = 1$) holds for perfect parallel alignment, $\gamma_0 = 54.5°$ ($S = 0$) holds for no such alignment, and $\gamma_0 = 90°$ ($S = -1/2$) holds for perfect vertical alignment with respect to the groove (orientation) direction:

$$S = \frac{(1 - R)}{(2R + 1)} \cdot \frac{2}{(3\cos^2\theta - 1)}, \tag{2}$$

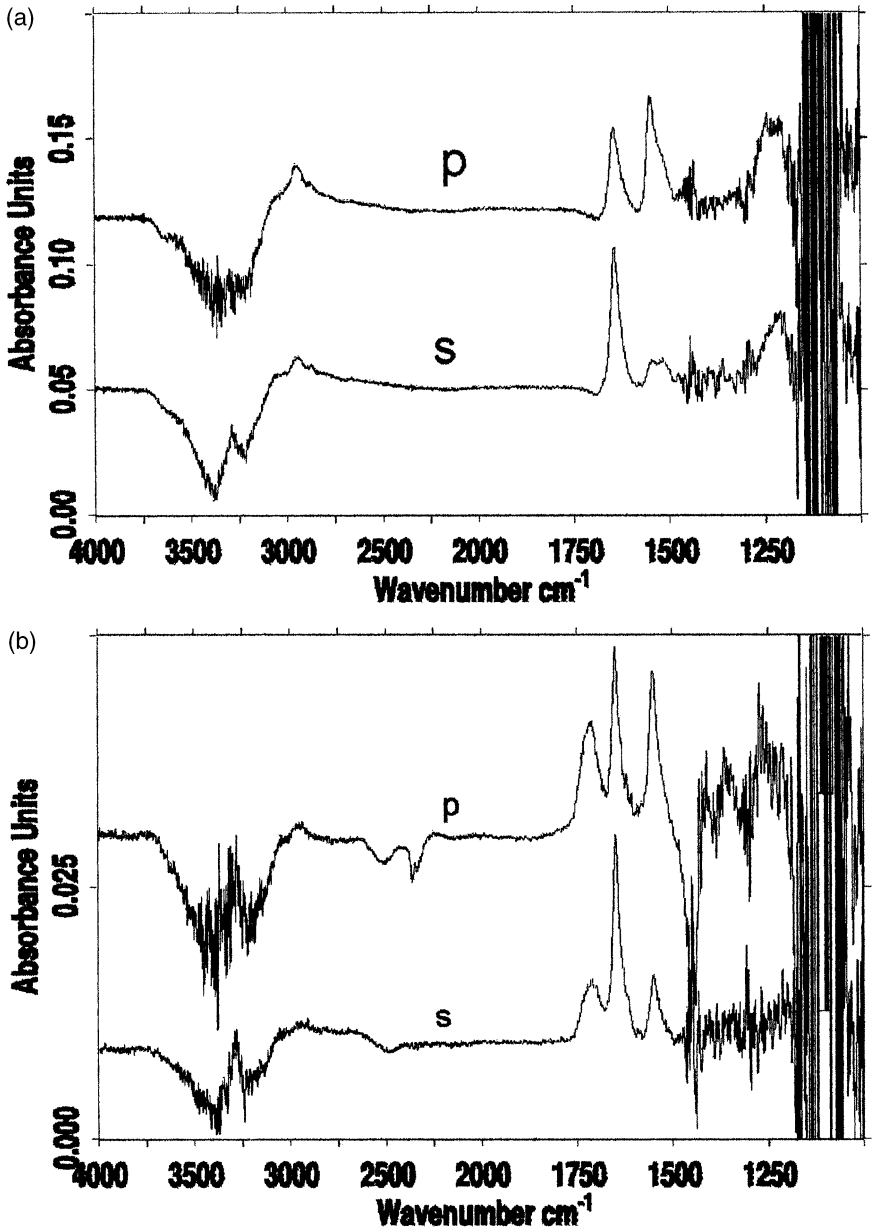

FIGURE 6 (a) p- and s-polarised ATR-FTIR spectra of a PEM-5 of α-PLL/PVS on texturized Si crystals (PLL M_w: 200.000 g/mol). (b) p- and s- ATR-FTIR polarisation spectra of PEM-4 of α-PLG/PDADMAC on texturized Si crystals (PLG M_w: 70.000 g/mol) (from Müller *et al.* [36], with kind permission of American Chemical Society).

TABLE 1 Experimental Values of R and Calculated Values of S and γ_0, Determined by Equations (2) and (3), on the Oriented and Unoriented PEMs of α-PLL/PVS (PEM-5) and α-PLG/PDADMAC (PEM-4)

	α-PLL/PVS (Amide I)		α-PLG/PDADMAC (Amide I)	
	Texturised	Untexturised	Texturised	Untexturised
R	0.39	0.72	0.54	0.75
S	0.79 ± 0.10	0.27 ± 0.10	0.51 ± 0.10	0.24 ± 0.10
$\gamma_0/[^\circ]$	22 ± 5	44 ± 5	35 ± 5	45 ± 5

Partly from Müller *et al.* [36], with kind permission of American Chemical Society.

$$\gamma_0 = \arccos\left(\sqrt{\frac{2}{3}S + \frac{1}{3}}\right). \tag{3}$$

In Table 1 the experimental dichroic ratios, R, the order parameters, S, and the cone opening angles, γ_0, are given for the PEMs of α-PLL/PVS and α-PLG/PDADMAC deposited at the untexturized and texturized substrate. Significantly, for the texturized case (S = 0.79, 0.51) an anisotropic arrangement of the α-helical PLL ($M_w = 200.000\,g/mol$) or PLG ($M_w = 70.000\,g/mol$) rods could be concluded, whereas for the untexturized case a minor orientation could be obtained (S = 0.27, 0.24) that also yet showed a small degree of preorientation on the Si support. From the values of Table 1 for the texturised case a PEM model can be derived in which the α-helical polypeptide rods are more or less assembled parallel within and out of the substrate grooves and the oppositely charged coiled PELs are acting as glue between the rods. This is further supported by Figure 7, where it can be shown that S becomes larger if the molecular weight of the PLL is increased from 20,000 to 300,000 g/mol [36]. This is caused by the elongation of the PLL macromolecule, since the contour length of the α-helix was increased from $L = 15-222\,nm$. Therefore, the growing aspect ratio forces the assembled α-helical polypeptide rods to a higher unidirectional alignment within the grooves of widths around $50-70\,nm$. As will be shown below, the surface of such PEMs offers interesting properties concerning the interaction with α-helical proteins.

Anisotropic PEM Surface Morphology

In Figure 8 the AFM micrograph of PEM-5 of PLL/PVS deposited onto texturized Si substrates is shown, where PLL was in the α-helical conformation, as shown above. Significantly, wormlike nanoscopic

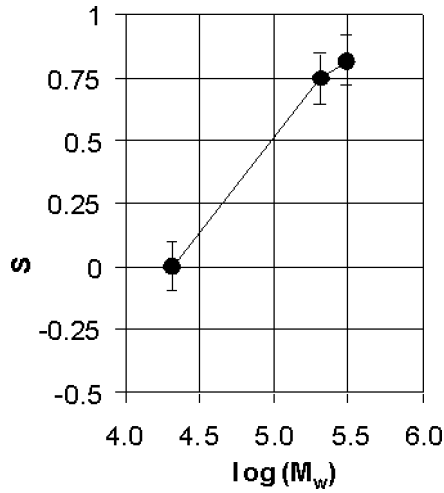

FIGURE 7 Order parameter S of α-helical PLL assembled in PEM-PLL/PVS as a function of the M_w. PLL, PVS solutions in the presence of 1 M $NaClO_4$ were used (S was based on R of the amide II band) (from Müller *et al.* [36], with kind permission of American Chemical Society).

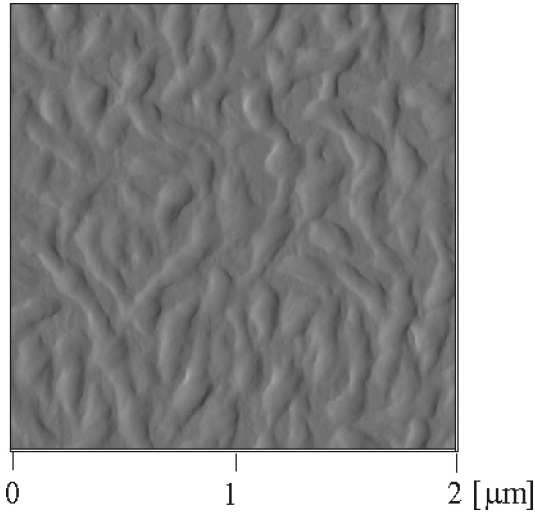

FIGURE 8 AFM micrograph of oriented PEM-5 of α-PLL (246.000 g/mol)/ PVS on (vertically to that line) texturized Si supports.

structures are visible on the surface, which are originated by the stiff α-helical PLL rods and that are further complexed with oppositely charged PVS. Furthermore, a preferential orientation of these nanoscopic wormlike structures with respect to the groove direction from bottom to top can be observed. Obviously, PEMs of stiff PELs may form anisotropic surface morphology in contrast to PEMs of flexible ones shown in Figure 4a.

Application Fields

Swellability

PEMs can be seen as *electrostatically crosslinked* hydrogel systems, which are highly sensitive to changes of the pH or the ionic strength of the aqueous environment [7]. In Figure 9a the swelling behavior of PEMs of PEI/PAC in contact with salt solutions having concentrations of $c_S = 0.1$, 0.5, 1, and 2 M is shown. Significantly, with growing salt concentration a diminuation of the ν(C=O)- and the $\nu(COO^-)$ band absorbance can be seen, which generally correlates with the diminuation of the polymer segment density or swelling. This trend was obtained for all three salt types NaCl, NaBr, and $NaClO_4$. Among them the strongest swelling was obtained in the case of the $NaClO_4$ solutions, since the perchlorate anion is known to bind tightly to ammonium cations. Consequently, fewer carboxylate groups of PAC are ion paired with the PEI ammonium groups, which leads to the observed swelling. Bromide and chloride anions are less expected to compete with the carboxylate groups, resulting in weaker swelling effects.

In Figure 9b the water uptake of PEMs of PEI and an alternating copolymer of maleic acid and α-methylstyrene (PMA-MS) from humid air (90% relative humidity) is illustrated. The ν(OH) band integral due to sorbed water normalized by the $\nu(COO^-)$ band integral due to the PEM adsorbed amount is plotted against the adsorption step. Interestingly, the PC-terminated PEMs (odd) showed the higher relative water sorption compared with the PA-terminated PEMs (even). Furthermore, this correlated with sessile drop measurements, where the PC-terminated PEM revealed the lower contact angle and thus the better wetting (advancing) compared with the PA-terminated PEM [26]. Both examples show the potential of PEMs as sensoric layers for mineral salt ions or for moisture.

Interactions with Proteins

PEMs are versatile platforms that are able to generate defined specific interaction to biochemical or biological compounds such as drugs,

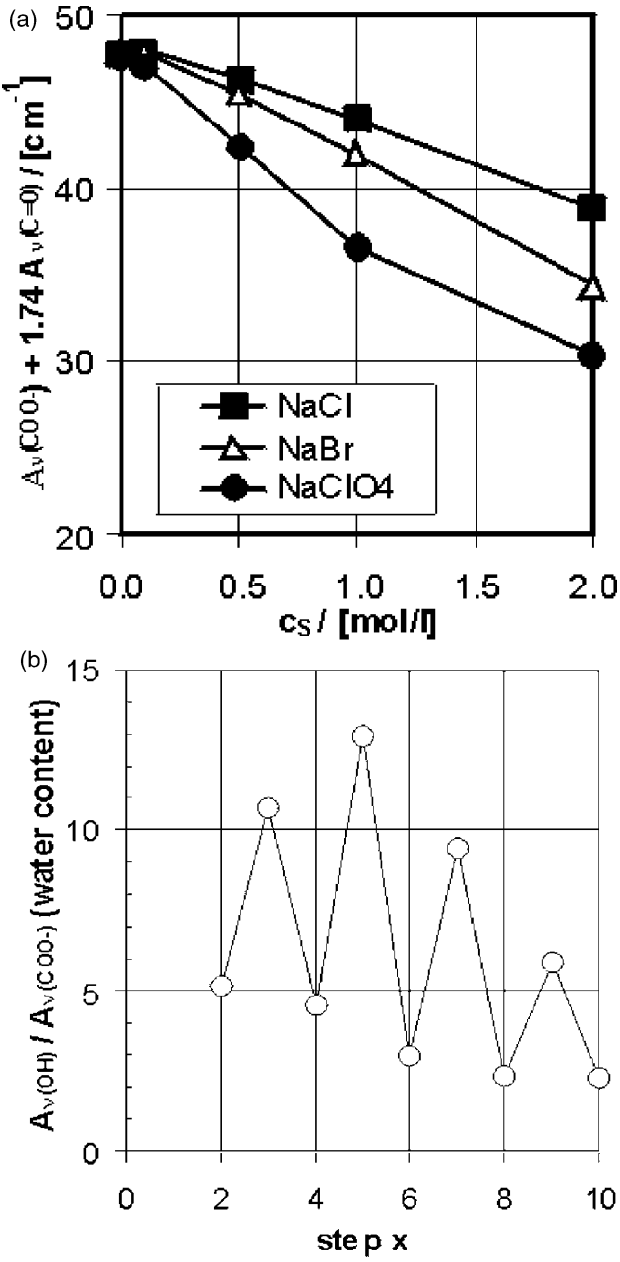

FIGURE 9 (a) Swelling of PEM-20 of PEI/PAC on Si supports monitored by the absorbance of the ν(C=O) and $\nu(COO^-)$ as a function of the concentration of the NaCl (■), NaBr (□), and $NaClO_4$ (○) contacting solution. (b)Water uptake of the PEM of PEI/PMA-MS from 90% relative humidity as a function of the adsorption step x. The ν(OH) band integral was normalized by that of the $\nu(COO^-)$ band (Partly from Müller [26], with kind permission of American Scientific Publishers).

peptides, proteins, genes, and cells *via* the outermost layer, and thus they are interesting for biomedical and pharmaceutical applications, as has been shown by several authors [15, 16, 42–47]. This can be achieved on the one hand by choice of the PC or the PA (charge sign), which effect electrostatic attraction or repulsion to, *e.g.*, ampholytic proteins. Additionally, using such biomimetic PEMs it is possible to mimick secondary structural elements such as the α-helix and β-sheet of target proteins by exposing polypeptides in the respective conformation in the outermost layer.

Electrostatic interactions. For studying electrostatic interactions between proteins and PEMs experiments on the adsorption of proteins at PEM-4 (-6) and PEM-5 of PEI/PAC on silicon supports have been performed using ATR-FTIR spectroscopy, which is highly sensitive due to the strong absorbing amide bands of proteins. Typical *in situ* ATR-FTIR spectra (amide band region) are shown in Figure 10 as a function of the adsorption time. Significantly, PEM-4 (PAC terminated, bottom) revealed only a minor adsorbed amount ($A_{\text{AMIDE I}} = 0.05\,\text{cm}^{-1}$) of human serum albumin (HSA), whereas the

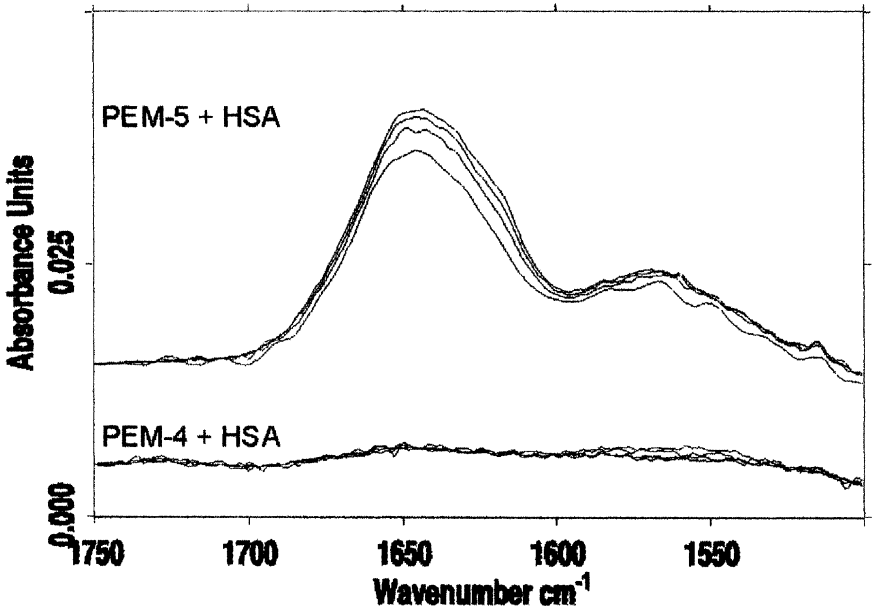

FIGURE 10 ATR-FTIR spectra on the adsorption of HSA (1 mg/ml, pH = 7.3, PBS buffer) at Si-ATR crystals modified by PEM-4 and PEM-5 of PEI/PAC (after 5, 15, 25, and 55 min from bottom to top, respectively).

PEM-5 (PEI terminated) showed a strong HSA adsorption ($A_{AMIDE\ I} = 1.01\,cm^{-1}$) at the PEM-5. Since a value of $A_{AMIDE\ I} = 0.7\,cm^{-1}$ corresponds to a monolayer surface coverage (HSA, $\Gamma_{MONO} \approx 0.20\,\mu g/cm^2$), less than 1/10 of Γ_{MONO} was adsorbed at the PEM-4. The protein resistance in the case of the PEM-4 was predominantly caused by electrostatic repulsion (a) between the outermost PAC layer and the acidic HSA due to an isoelectric point IEP = 4.8 at pH = 7.3. For other proteins the adsorbed amounts at the oppositely charged PEM surface was shown to scale with the deviation between their IEP and the pH [17].

Nonelectrostatic interactions. For bioactive materials or diagnostics, biosensors surfaces that bind certain proteins and peptides selectively are useful. For example, Huber *et al.* [48] developed biosensor systems by which the specific binding between cell wall glycoproteins and fibrinogen and their potent inhibition can be measured as a function of time. There the recognition of defined peptide sequences (Arg-Gly-Asp) was found. On the other hand, alternative concepts are interesting for creating bioninert surfaces besides the known ones of, *e.g.*, hydrogel layers (PEG [49], PHEMA [50]), diamond-like carbons [51], phospholipid-containing polymers [52], or charge repulsion (previous section) and others. A new aspect could be the use of nonnatural biopolymers. In that framework we were interested whether there is a difference in the interaction of natural proteins with homopolypeptides composed of amino acids in the L-form compared with those containing amino acids in the D-form. For that model, adhesion experiments of the α-helical rich myoglobin (MYO) were performed at the PEM-5 consisting of α-helical PLL (α-PLL) and PVS (i) and at the analogous PEM-5 of α-PDL/PVS (ii). In both PEM-5 (i) and PEM-5 (ii), PLL and PDL were exposed in the outermost layer at pH = 7.3, where MYO should be approximately uncharged (IEP ≈ 7). The result is shown in Figure 11, where the PEM-5 terminated by α-PLL and that terminated by α-PDL revealed approximately the same adsorbed amount of MYO after 150 min of adsorption time. Obviously, in that case no specific recognition of MYO by the immobilized polypeptide layer on the configurational (chirality) level took place.

Membrane Applications

Prevention of Fouling

Membranes, as they are applied in the water, beverage, and pharmaceutical industry, can still be improved with respect to flux, separation, and nonfouling properties. In that framework the PEM concept

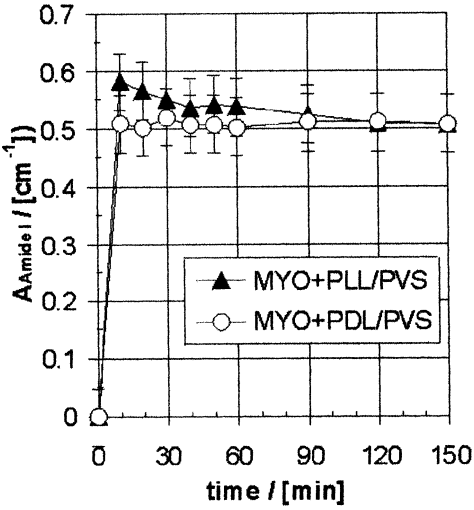

FIGURE 11 Adsorption kinetics of MYO (1 mg/ml, pD = 7.3, PBS buffer) at the PEM-5 of PLL/PVS (▲) and that of PDL/PVS (○) exposing the polypeptide in the α-helical conformation.

can be used to control the surface energy and charge of microporous membranes in a defined manner. Especially the membrane fouling, for which hydrophobic as well as electrostatic interactions play a major role, can be influenced by PEM deposition within the membrane. Recent articles on that topic [53–58] describe the interaction of PEMs, which are consecutively adsorbed at hydrophobic polymer membranes (*e.g.*, polypropylene), with model protein solutions and natural organic matter (NOM). In a grafting reaction of acrylate monomers a first PAC layer can be deposited, onto which PEMs of PC/PAA can be further anchored. Microporous polypropylene membranes (Celgard 2400, Hoechst AG, Germany; pore size $120 \times 40\,nm^2$, porosity 28–40%) were used as support for the PEMs. The modification was carried out in three distinctive steps: (1) activation of the polypropylene PP surface by CO_2-plasma treatment resulting in the formation of peroxide species; (2) grafting of charged monomers, *e.g.*, acrylic acid, onto the Polypropylene PP surface from aqueous monomer solution by thermal decomposition of the peroxides; and (3) adsorption of additional PEL using the dip coating process described by Decher *et al*. [5]. As is shown in Figure 12, this caused a decreased adsorption of HSA in comparison with the unmodified and the plasma-modified membrane samples (first and second bars in

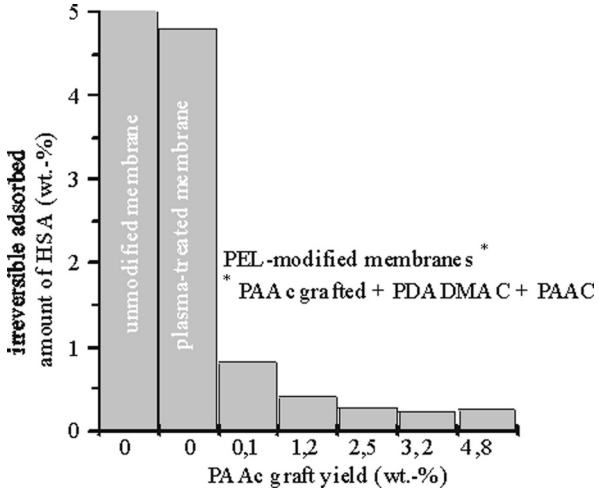

FIGURE 12 Influence of the PEM modification and the grafting degree on the irreversible fouling, *i.e.*, HSA adsorption, at polypropylene membranes (pH = 6.5) (from Meier-Haack *et al.* [55], with kind permission of Springer).

Figure 12). The bars 3–7 show the significant decrease of adsorbed HSA amount using two more consecutive layers of PC and PA, which caused electrostatic repulsion between protein and surface, as was explained with the PEM deposited on planar Si substrates above. The irreversibly adsorbed amount of HSA on graft-modified membranes without PEM is slightly higher than that of PEM modified membranes. However, the permeate flux is only half that of PEM-modified membranes [59]. An additional diminution is seen with an increasing degree of grafting (0.1–4.8 wt%) of the PAC base layer due to increasing hydrophilic surface coverage of the base layer. Furthermore, by the PEM concept elevation of the membrane flux ([36], data not shown) was achieved, caused by the enhanced hydrophilicity of the membrane surface and conformational changes of the first grafted layer due to complex formation. In further studies it has been shown that a certain graft yield for the first PEL layer, depending on the pore size of the substrate, is necessary, to achieve an antifouling effect, accompanied with an enhanced rejection during protein filtration [60], and the membranes can be easily cleaned by rinsing with pure water. The protein molecules stick to the unmodified "inner surface" of the membrane while passing through the membrane with the permeate stream. In other words, fouling by protein adsorption takes place not only at the "outer surface" but also at the "inner surface."

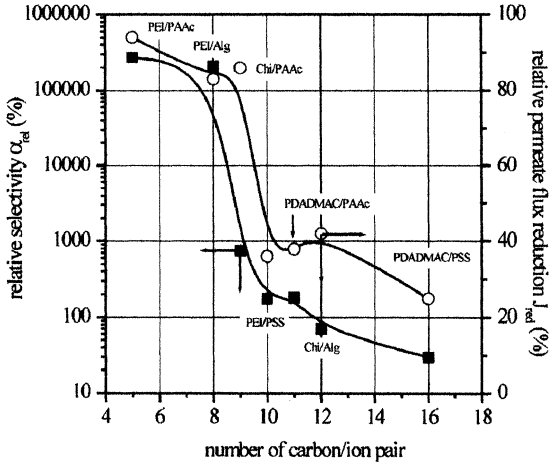

FIGURE 13 Effect of PEL pairs on membrane properties used in separation of water/2-propanol (30/70 wt/wt @ 50°C). Six double layers were deposited on a polyamide-6 support. $\alpha_{rel} = \alpha_{PEL}/\alpha_0{}^*100\%$, and $J_{red} = J_{PEL}/J_0{}^*100\%$. (from Berwald and Meier-Haack [56], with kind permission of American Scientific Publishers).

Upon grafting, the pore size is reduced so that the protein molecules are hindered in entering the membrane.

Dense Membranes

The first membranes that were prepared using the layer-by-layer technique have been described in the literature by Stroeve *et al.* [61] and Leväsalmi, McCarthy [62]. The membranes were used in gas-separation applications. However, the selectivities based on single gas permeabilities were less than those observed for conventional gas separation membranes. A second approach to utilize dense membranes prepared by PEM systems for pervaporation was achieved by van Ackern *et al*. and other authors [13, 63–65]. These membranes were used for the separation of aqueous organic mixtures to overcome the azeotropic point, *e.g.*, dewatering of alcohols by pervaporation, as ion-selective nanofiltration membranes [66–68] as well as in chiral separations [69]. The separation capabiltily is strongly affected by the polyelectrolytes used for the PEM buildup [56, 64], the layer number, and the preparation conditions (salt content, pH, temperature, etc.). As a result, dense PEM membranes from PELs with a high "charge density" (in terms of the number of *C-atoms/ion pair* in the repeating unit) *e.g.*, poly(acrylic acid)/poly(ethylene imine), showed

highest separation and lowest permeate flux, while those prepared from PEL with low "charge density" had a high permeate flux and low separation properties (Figure 13). Contrary to the preparation procedure described in early works of PEM membranes [63, 64], the pH of the PEL solutions was not adjusted. The pH of the PAC solution was approximately 3.5 and that of the PEI solution was around 9.0. Hence, according to the pK_A and pK_B, values of the respective PELs there are dissociated and nondissociated functional groups present in the polymer chain. The improved separation properties of these membranes can be attributed to the fact that the partially charged PELs are adsorbed in a more disordered state than the highly charged PELs, but the layers themselves are thicker, as in the latter case, and a complete coverage of the support surface is achieved at a smaller number of deposited layers.

A high impact of preparation conditions on the membrane properties was observed when the deposition temperature was raised from 25°C to 80°C [65]. The selectivity of membranes prepared at 80°C was *ca.* 500 times higher than for that prepared at 25°C. However, this strong increase in selectivity was accompanied by a decreasing permeate flux.

As outlined in Table 2, dense PEM membranes are not only suitable to separate water–alcohol mixtures but also other aqueous–organic mixtures.

The layer-by-layer technique was also used to modify Nafion®-117 membranes, which are widely used in fuel cell applications. One disadvantage of the Nafion membranes is the high methanol crossover when used in direct methanol fuel cells (DMFC), which leads to undesired side reaction at the cathode. The modification of Nafion®

TABLE 2 Separation Properties of PEM Membranes Based on Six Layer Pairs Consisting of PEI/PAC

Test mixture	Composition of the feed mixture (wt%)	Separation factor, α	Permeate flux, J (kg/m^2h)
Water/2-Propanol	30/70	3330	0.67
Water/2-Propanol	75/25	2000	0.74
Water/Ethanol	22/78	2340	0.21
Water/Ethanol	10/90	1400	0.02
Water/Methanol	13/87	75	0.04
Water/Methanol	89/11	17	1.20
Water/Tetrahydrofuran	13/87	61000	0.62
Water/Dimethylacetamide	30/70	860	0.51

Pervaporation temperature, 50°C.

From Meier-Haack *et al.* [13], with kind permission of Elsevier.

TABLE 3 Results of Pervaporation Experiments with Unmodified and PEL-Modified Nafion® Membranes

Preparation temp. (°C)	Layer number PEI/PAC	MeOH in the feed (wt%)	MeOH in the permeate (wt%)	Permeate flux (kg/m^{2}h)	Operating temp. (°C)
pure	2/2	10	13	5.8	50
pure	2/2	29	31	4.7	50
25	2/2	9	2	5.9	80
25	2/2	26	13	5.5	80
80	2/2	11	0.02	1.0	80
80	2/2	24	0.12	0.9	80

From Meier-Haack and Müller [53], with kind permission of Wiley-VCH.

membranes with PELs, especially at higher temperatures, resulted in a dramatic enhancement of water selectivity (Table 3). Such membranes showed high stability and high methanol retention when tested in direct methanol fuel cells. However, the electrical properties were poorer than those of unmodified Nafion® membranes. Nontheless, PEM assemblies seemed to be promising materials for proton conductive membranes in fuel cell applications.

CONCLUSION

An overview of our recent results concerning the PEM surface modification concept was given. Exemplary results on the characterization of various PEM systems by a variety of surface analytical tools were given. PEMs were shown to be built up and to be controlled in a defined way by macromolecular structural parameters such as molecular weight and chain flexibility, as well as by parameters of the aqueous medium like ionic strength and pH. Furthermore, PEMs were shown to function as versatile platforms to achieve distinct active (binding), release, inert, hydrophilization, and separation properties in several applications.

REFERENCES

[1] Horn, D., and Linkart, F., *Retention Aids* in Paper Chemistry, Roberts, J. (Ed.) (Blackie, Glasgow, 1999) Chapter 4, pp. 64–82.
[2] Wagberg, L. and Kolar, K., *Ber. Bunsen Ges. Phys. Chem*. **100**, 984 (1996).
[3] Mir, Y., Auroy, P., and Auvray, L., *Phys. Rev. Lett.* **75**, 2863 (1995).
[4] Biesalski, M. and Rühe, J., *Macromolecules* **32**, 2309 (1999).
[5] Decher, G., Hong, J. D., and Schmitt, J., *Thin Solid Films* **210**/**211**, 831 (1992).
[6] Bertrand, P., Jonas, A., Laschewsky, A., and Legras, R., *Macromol. Rapid Commun.* **21**, 319 (2000).

[7] Schönhoff, M., *J. Phys.: Condensed Matter* **15**, 1781 (2003).
[8] Buchhammer, H. M., Petzold, G., and Lunkwitz, K., *Langmuir* **15**, 4306 (1999).
[9] Buchhammer, H.-M., Mende, M., and Schwarz, S., *Prog. Colloid Polym. Sci.* (submitted).
[10] Mende, M., Petzold, G., and Buchhammer, H.-M., *Colloid Polymer Sci.* **280**, 342–351 (2002).
[11] Reihs, T., Müller, M., and Lunkwitz, K., *Coll. Surf. A* **212**, 79 (2003).
[12] Reihs, T., Müller, M., and Lunkwitz, K., *J. Coll. Interf. Sci.* **271**, 69–79 (2004).
[13] Meier-Haack, J., Lenk, W., Lehmann, D., and Lunkwitz, K., *J. Membr. Sci.* **184**, 233 (2001).
[14] Meier-Haack, J. and Müller, M., *Macromol. Symp.* **188**, 91 (2002).
[15] Müller, M., Rieser, T., Lunkwitz, K., Berwald, S., Meier-Haack, J., and Jehnichen, D., *Macromol. Rapid Commun.* **19**, 333 (1998).
[16] Müller, M., Brišš**ová**, M., Rieser, T., Powers, A. C., and Lunkwitz, K., *Mat. Sci. Eng.* **C8-9**, 167 (1999).
[17] Müller, M., Rieser, T., Dubin, P., and Lunkwitz, K., *Macromol. Rapid Commun.* **22**, 390 (2001).
[18] Schwarz, S., Nagel, J., and Jaeger, W., *Macromol. Symp.* **211**, 201–216 (2004).
[19] Fringeli, U. P., In: *Encyclopedia of Spectroscopy and Spectrometry*, Lindon, J. C., Tranter, G. E., and Holmes, J. L., Eds. (Academic Press, New York, 2000) pp. 58–75.
[20] Decher, G., *Science* **277**, 1232 (1997).
[21] Ladam, G., Schaad, P., Voegel, J. C., Schaaf, P., Decher, G., and Cuisinier, F., *Langmuir* **16**, 1249 (2000).
[22] Castelnovo, M. and Joanny, J. F., *Langmuir* **16(19)**, 7524 (2000).
[23] Müller, M., *Biomacromolecules* **2**, 262 (2001).
[24] Kleinfeld, E. R. and Ferguson, G. S., *Science* **265**, 370 (1994).
[25] Arys, X., Laschewsky, A., and Jonas, A. M., *Macromolecules* **34**, 3318 (2001).
[26] Müller, M., In: *Handbook of Polyelectrolytes and Their Applications*, Tripathy, S. K., Kumar, J., and Nalwa, H. S., Eds. (American Scientific Publishers, Stephenson Ranch, CA, 2002), Vol. 1, pp. 293–312.
[27] Thünemann, A. F., Müller, M., Dautzenberg, H., Joanny, J. F., Löwen, H., Polyelectrolyte Complexes, In *Advances in Polymer Science*, Vol. 166, M. Schmidt (Ed.), (Springer, 2004), pp. 113–171.
[28] Schaaf, P., Dechardin, P., and Schmitt, A., *Langmuir* **3**, 1131 (1987).
[29] Dubas, S. T., and Schlenoff, J. B., *Langmuir* **17**, 7725 (2001).
[30] Cooper, T. M., Campbell, A. L., and Crane, R. L., *Langmuir* **11**, 2713 (1995).
[31] Araki, K., Wagner, M. J., and Wrighton, M. S., *Langmuir* **12**, 5393 (1996).
[32] Linford, M. R., Auch, M., and Möhwald, H., *J. Amer. Soc.* **120**, 178 (1998).
[33] Dragan, S., Schwarz, S., Eichhorn, K. J., and Lunkwitz, K., *Coll. & Surf. A* **195**, 243–251 (2001).
[34] Dragan, S. and Schwarz, S., *Macromol. Symp.* **181**, 155–166 (2002).
[35] Schwarz, S., Eichhorn, K.-J., Wischerhoff, E., and Laschewsky, A., *Coll. & Surf. A* **159**, 491–501 (1999).
[36] Müller, M., Kessler, B., and Lunkwitz, K., *J. Phys. Chem.* **107**, 8189 (2003).
[37] Boulmedais, F., Schwinte, P., Gergely, C.,Voegel, J.-C., and Schaaf, P., *Langmuir* **18(11)**, 4523–4525 (2002).
[38] Debreczeny, M., Ball, V., Boulmedais, F., Szalontai, B., Voegel, J.-C., and Schaaf, P., *J. Phys. Chem. B*.**107(46)**, 12734–12739 (2003).
[39] Boulmedais, F., Ball, V., Schwinte, P., Frisch, B., Schaaf, P., and Voegel, J.-C., *Langmuir* **19(2)**, 440–445 (2003).
[40] Marsh, D., Müller, M. and Schmitt, F. J., *Biophys. J.* **78**, 2499 (2000).

[41] Zbinden, R., *IR-Spectroscopy of High Polymers* (Academic Press, NY, 1964).
[42] Chluba, J., Voegel, J.-C., Decher, G., Erbacher, P., Schaaf, P., and Ogier, J., *Biomacromolecules* **2(3)**, 800–805 (2001).
[43] Brynda, E. and Houska, M., *J. Coll. Interf. Sci*. **183**, 18–25 (1996).
[44] Brynda, E., Houska, M., Jirouskova, M., and Dyr, J. E., *J. Biomed. Mater. Res*. **51**, 249–257 (2000).
[45] Schwinte, P., Voegel, J. C., Picart, C., Haikel, Y., Schaaf, P., and Szalontai, B., *J. Phys. Chem. B* **105(47)**, 11906 (2001).
[46] Szyk, L., Schwinte, P., Voegel, J. C., Schaaf, P., and Tinland, B., *J. Phys. Chem. B*. **106(23)**, 6049–6055 (2002).
[47] Jessel, N., Atalar, F., Lavalle, P., Mutterer, J., Decher, G., Schaaf, P., Voegel, J.-C., and Ogier, J., *Advanced Materials* **15(9)**, 692–695 (2003).
[48] Huber, W., Hurst, J., Schlatter, D., Barner, R., Hübscher, J., Kouns, W. C., and Steiner, B., *Eur. J. Biochem.* **227**, 647 (1995).
[49] Desai, N. P. and Hubbell, J. A., *Biomaterials* **12**, 144 (1991).
[50] Peppas, N. A., Moynihan, H. I., and Lucht, L. M., *J. Biomed. Mater. Res*. **19**, 397 (1985).
[51] Higson, S. P. J. and Vadgama, P. M., *Anal. Chim. Acta* **271**, 125 (1993).
[52] Ishihara, K., Nomura, H., Mihara, T., Kurita, K., Iwasaki, N., and Nakabayashi, N., *J. Biomed. Mater. Res*. **39**, 323 (1997).
[53] Meier-Haack, J. and Müller, M., *Macromol. Symp.* **188**, 91–104 (2002).
[54] Rieser, T., Lunkwitz, K., Berwald, S., Meier-Haack, J., Müller, M., Cassel, F., Dioszeghy, Z., and Simon, F., In: *Membranes Formation and Modification* ACS Symposium Series, **744**, Ingo Pinnau, Ed. (ACS, Washington, DC, 1999), Chap. 13.
[55] Meier-Haack, J., Müller, M., and Lunkwitz, K., In: *Polymers: Chances and Risks*, Eyerer, P., Kröner, S., and Weller, M., Eds. (Springer Verlag, Heidelberg) submitted.
[56] Berwald, S. and Meier-Haack, J. In: *Handbook of Polyelectrolytes and Their Applications*, Tripathy, S. K., Kumar, J., and Nalwa, H. S., Eds. (American Scientific Publishers, Stephenson Ranch, CA, 2002), Vol. 3, pp. 99–114.
[57] Carroll, T., Booker, N. A., and Meier-Haack, J. *J. Membr. Sci.* **203**, 3–13 (2002).
[58] Meier-Haack, J., Booker, N. A., and Carroll, T., *Water Res.* **37**, 585–588 (2003).
[59] Rieser, T., Modifizierung von mikroporösen Polypropylenmembranen mit Polyelektrolyten und Polyelektrolytkomplexschichten, PhD Thesis, Dresden Technical University (TUD), Dresden (1999).
[60] Endres, A., Modifizierung von Polypropylen–Hohlfasermembranen für die Trinkwasseraufbereitung und ihre Charakterisierung, Diploma Thesis, University of Applied Sciences (HTW), Dresden (2003).
[61] Stroeve, P., Vasquez, V., Coelho, M. A. N., and Rabolt, J. F., *Thin Solid Films* **284–285**, 708–712 (1996).
[62] Leväsalmi, J. and McCarthy, T. J., *Macromolecules* **30**, 1752–1757 (1997).
[63] van Ackern, F., Krasemann, L., and Tieke, B., *Thin Solid Films* **327–329**, 762 (1998).
[64] Krasemann, L. and Tieke, B., *Mater. Sci. Eng.* **C8–9**, 513–518 (1999).
[65] Lenk, W. and Meier-Haack, J., *Desalination* **148**, 11–16 (2002).
[66] Jin, W., Toutianoush, A., and Tieke, B., *Langmuir* **19**, 2550–2553 (2003).
[67] Bruening, M. L., Stanton, B., Liu, X., and Harris, J. J., *Polymeric Mater. Sci. Eng.* **89**, 169 (2003).
[68] Balachandra, A. M., Dai, J. H., and Bruening, M. L., *Macromolecules* **35**, 3171–3178 (2002).
[69] Rmaille, H. H. and Schlenoff, J. B., *J. Am. Chem. Soc.* **125**, 6602–6603 (2003).